

## ALTERNATIVE CAPTIVE MANOEUVRING TESTS: POSSIBILITIES AND LIMITATIONS

Katrien ELOOT

University of Ghent (Department of Applied Mechanics, Section Maritime Technology), Technologiepark Zwijnaarde 9, B 9052 Gent, Belgium

Marc VANTORRE

University of Ghent (Department of Applied Mechanics, Section Maritime Technology) — Fund for Scientific Research - Flanders  
c/o Flanders Hydraulics, Berchemlei 115, B 2140 Antwerpen, Belgium

### ABSTRACT

Computational techniques and empirical data do not yet allow determination of a mathematical manoeuvring model for a specific ship in rather extreme conditions, such as harbour manoeuvres in very shallow and restricted water. Therefore, experimental techniques, and in particular the execution of captive manoeuvring tests, will keep fulfilling an important task for several purposes. Time consuming series of stationary model tests are compared to alternative non-stationary captive model tests during which several test parameters are varied continuously with the view to obtaining all information needed in a limited number of test runs. Considering the difficulties related to the determination of mathematical models for the simulation of harbour manoeuvres, the authors intend to report on a first evaluation of the possibilities and limitations of these alternative captive model tests, rather than presenting a completely innovative PMM test procedure.

### NOMENCLATURE

$a_H$	ratio between lateral forces on rudder and hull	(-)
$B$	Breadth of ship/model	(m)
$C_B$	Block coefficient	(-)
$D$	Propeller diameter	(m)
$h$	Water depth	(m)
$L_{pp}$	Length between perpendiculars of ship/model	(m)
$n$	Propeller rate	(rpm)
$N$	Yawing moment	(Nm)
$r$	Yaw velocity	(rad/s)
$\dot{r}$	Yaw acceleration	(rad/s <sup>2</sup> )
$t$	Time	(s)
$T$	Draught of ship/model	(m)
$T$	Period	(s)
$u$	Longitudinal component of velocity $V$	(m/s)
$\dot{u}$	Longitudinal acceleration component	(m/s <sup>2</sup> )
$v$	Lateral component of velocity $V$	(m/s)
$\dot{v}$	Lateral acceleration component	(m/s <sup>2</sup> )
$V$	magnitude of speed vector $V=(u^2+v^2)^{1/2}$	(m/s)
$x_H$	longitudinal position of the application point of the lateral force acting on the hull	(m)
$x_R$	longitudinal position of the application point of the lateral force acting on the rudder	(m)
$X$	Longitudinal force	(N)
$Y$	Lateral force	(N)
$Y_R$	Lateral force acting on the rudder	(N)
$\beta$	Drift angle $\beta = \arctan(-v/u)$	(deg)
$\gamma$	Hydrodynamic inflow angle $\gamma = \arctan(rL/2u)$	(deg)
$\delta$	Rudder angle	(deg)
$\phi$	Phase angle	(deg)
$\omega$	Oscillation frequency $\omega = 2\pi/T$	(rad/s)
Subscripts:		
$m$	mean (average) value	
$A$	amplitude	

### 1. INTRODUCTION

The determination of a reliable mathematical model for simulating manoeuvres under rather extreme conditions, like harbour manoeuvres at slow speed in shallow and restricted water assisted by tug boats, is an important topic and demanding task for research groups and international organizations involved with the issue of design of harbour facilities and waterways. Up till now, the most reliable method for collecting the input data required for such simulation studies appears to be the execution of captive manoeuvring tests in a towing tank or circulating water channel.

The hydrodynamic forces and moments acting on a manoeuvring ship depend on a number of kinematical parameters (velocity and acceleration components in surge, sway and yaw) and control parameters (rudder angle, propeller rate):

$$\begin{aligned} X &= f_1(n, v, r, u, v, r, \delta, n) \\ Y &= f_2(u, v, r, u, v, r, \delta, n) \\ N &= f_3(u, v, r, u, v, r, \delta, n) \end{aligned} \quad (1)$$

Due to the complex interaction between the different components of a manoeuvring vessel (hull, propeller and rudder), the required number of captive manoeuvring tests, and, consequently, the total test duration, can be very large, especially if manoeuvres characterized by a large broad range of drift angles  $\beta$ , forward speeds and propeller actions have to be simulated.

If the captive model tests are executed by means of a computer controlled planar motion mechanism (PMM), it is principally possible to replace a series of 'traditional' stationary tests (rudder angle tests, oblique towing tests) by a few 'alternative tests' during which several test parameters are varied simultaneously, so that a large number of combinations can be covered in a limited number of runs.

The present paper intends to focus on the possibilities and limitations of these alternative captive manoeuvring tests by comparing their results with the output of more generally applied stationary captive model tests.

## 2. EXPERIMENTAL TECHNIQUE

### 2.1. Multimodal tests

In order to realize a large number of parameter combinations during one run, so-called 'multimodal' tests were introduced, during which one or more kinematical or control parameters  $f$  are varied as harmonic functions of time:

$$f(t) = f_m + f_A \sin(\omega_f t + \phi_f) \quad (2)$$

Mean value  $f_m$ , oscillation amplitude  $f_A$ , pulsation  $\omega_f$  (or period  $T_f$ ) and phase angle  $\phi_f$  can be chosen independently for each kinematical parameter ( $f = u, v, r$ ) or control parameter ( $f = n, \delta$ ).

Harmonic PMM sway and yaw tests can be considered as multimodal tests where the lateral velocity  $v$  and the yaw rate  $r$ , respectively, are varied as harmonic time functions, while the other test parameters are kept constant. Combined oscillatory tests, referred to by Rhee [1], can be considered as another particular example of multimodal tests. However, the purpose of PMM tests consists in imposing harmonic sway and yaw accelerations to a ship model, rather than combining ranges of test parameters.

It should be born in mind that, during all tests with a harmonic character, the test parameters are varied in a non-stationary way, although the test results will be applied in a quasi-stationary mathematical manoeuvring model. Previous research showed that, especially in shallow water, the results of such non-stationary tests may be characterized by the occurrence of memory effects (Vantorre and Elout [2]).

Therefore, if non-stationary multimodal tests will be introduced in a standard PMM test procedure in order to reduce the number of stationary tests required to predict the manoeuvring performance of a vessel, this should be done with the greatest caution, as the introduction of non-stationary phenomena should be avoided as much as possible.

### 2.2. Test conditions.

The experimental observations are based on an extensive test program, executed with several slender and full form ship models at different depth-to-draught ratios  $h/T$ . The selected test series referred to in this paper are summarized in table 1; all tests were carried out in very shallow water ( $h/T \leq 1.2$ ).

The experiments were carried out at the *Towing Tank for Manoeuvres in Shallow Water* (cooperation Flanders Hydraulics - University of Ghent), Antwerp (Belgium), a basin with length 88 m, width 7 m and maximum water depth 0.5 m, equipped with a fully computer controlled (x,y, $\psi$ )-carriage. The fully automated, unmanned mode allows execution of about 30 tests a day, even if large waiting times (30 - 40 minutes) have to be respected, as is the case in shallow water.

Table 1. Test conditions and model characteristics

Test series	ship type	h/T	scale	$L_{pp}$ (m)	B (m)	T (m)	$C_B$ (-)
C2	bulk	1.10	1/64	235.0	32.24	12.25	0.828
C3	bulk	1.10	1/64	220.0	32.24	12.25	0.811
DB	cont	1.13	1/75	289.8	40.25	15.00	0.609
FA	cont	1.17	1/50	190.0	32.00	11.60	0.601
GA	bulk	1.17	1/50	180.0	33.00	11.60	0.840
GE	bulk	1.19	1/50	180.0	33.00	13.00	0.847

### 2.3. Test program

Following types of multimodal tests will be discussed in this paper:

- combinations of drift and propeller action, with the purpose of reducing the number of oblique towing tests under varying propeller loading;
- combinations of drift and yaw, with the purpose of replacing a comprehensive series of oblique towing tests by a limited number of multimodal tests;
- combinations of propeller and rudder actions, in order to reduce the number of straight or oblique towing tests with rudder action under varying propeller loading.

## 3. DRIFT WITH VARIABLE PROPELLER ACTION

### 3.1. Mathematical model

Contrary to manoeuvres at medium or full speed, a mathematical model suited for the simulation of harbour manoeuvres at low and even reversed speed should contain expressions for the lateral force and the yawing moment as a function of drift angle which cover four quadrants ( $-180 \text{ deg} < \beta < 180 \text{ deg}$ ).

A comprehensive evaluation of formulations for the hydrodynamic forces due to drift, summarized in Vantorre and Elout [3], led to the conclusion that the most reliable and accurate formulation of these forces and moments requires the introduction of a tabular representation for the non-dimensional lateral force  $Y'$  and yawing moment  $N'$  as function of drift angle  $\beta$

$$Y'(\beta, 0) = \frac{Y(\beta, 0)}{\frac{1}{2} \rho V^2 L^2}; \quad N'(\beta, 0) = \frac{N(\beta, 0)}{\frac{1}{2} \rho V^2 L^3} \quad (3)$$

Expressions (3) are valid in the case of pure drift without propeller action ( $n=0$ ). In order to take account of the influence of propeller action on  $Y'$  and  $N'$ , expressions (4) and (5) were proposed for the case of positive propeller rate ( $n$

> 0), based on the assessment that the flow circulation around the ship is apparently extended aft of the ship due to propeller action, which can be interpreted as an extension of the ship length  $L$ :

$$Y'(\beta, n) = \left[ 1 + C(\beta) \left( \frac{n}{n_{\max}} \right)^2 \right] Y'(\beta, 0) \quad (4)$$

$$N'(\beta, n) = N'(\beta, 0) + C(\beta) \left( \frac{n}{n_{\max}} \right)^2 \left( \frac{x_Y}{L} \right) Y'(\beta, 0) \quad (5)$$

The coefficient  $C(\beta)$  and the non-dimensional application point of the propeller induced force  $x_Y/L$  are presented as tables of  $\beta$  as well.

In order to assure continuity of the data, the tables should contain values for following 30 drift angles:  $0, \pm 2.5, \pm 5, \pm 10, \pm 15, \pm 20, \pm 30, \pm 60, \pm 90, \pm 120, \pm 150, \pm 160, \pm 170, \pm 175, \pm 177.5, 180$  deg. It is clear that larger drift angles can only be investigated at very low speed ( $F_n \approx 0.02$ ).

### 3.2. Stationary tests

Each test run of a stationary oblique towing test with propeller action is characterized by:

- a constant model speed  $V$  or Froude number  $F_n$ ;
- a constant drift angle  $\beta$ ;
- a discrete number of propeller rates ( $n_1, n_2, \dots, n_m$ ), each one being kept constant during a fraction of the total test length.

It was experienced that in shallow water a measuring length of 3 to 4  $L$  per condition can be considered as a minimum; at Flanders Hydraulics, this implies that three propeller rates can be applied per run, taking account of the usual model length ( $\approx 4$  m) and the available tank length ( $\approx 65$  m).

### 3.3. Multimodal test

Each test run of a multimodal oblique towing test with variable propeller action is characterized by:

- a constant model speed  $V$  or Froude number  $F_n$ ;
- a constant drift angle  $\beta$ ;
- a harmonic oscillating propeller rate

$$n(t) = n_m + n_A \sin(\omega_n t + \phi_n) \quad (6)$$

The advantage of the latter test type is the large amount of parameter combinations ( $\beta, n$ ), which principally only depends on the time step  $\Delta t$  of the measurements.

Although reversed propeller action was investigated as well (see 3.5), only multimodal tests carried out at positive propeller rate were considered for comparison with oblique towing tests. During these tests,  $n_m = n_A = \frac{1}{2} n_{\max}$ , so that the full range of propeller action ahead is applied.

Figure 4 (right) : Comparison between the non-dimensional application point  $x_Y/L$  resulting from stationary and multimodal tests (GE).

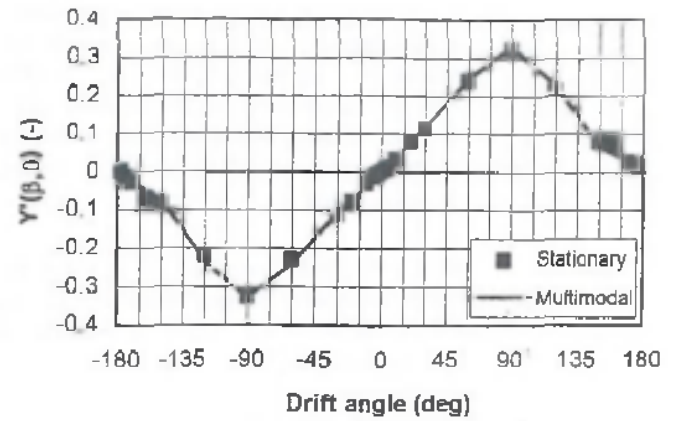


Figure 1: Comparison between the non-dimensional lateral force  $Y'(\beta, 0)$  due to drift without propeller action resulting from stationary and multimodal tests (GE).

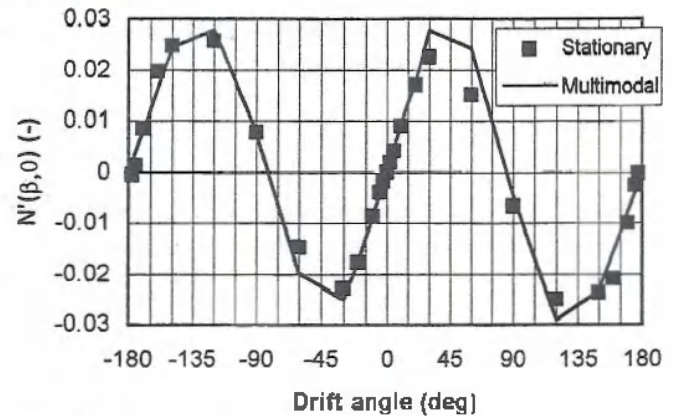


Figure 2: Comparison between the non-dimensional yawing moment  $N'(\beta, 0)$  due to drift without propeller action resulting from stationary and multimodal tests (GE).

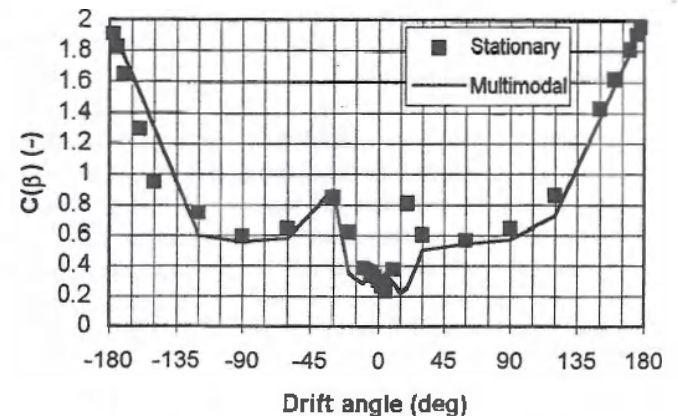
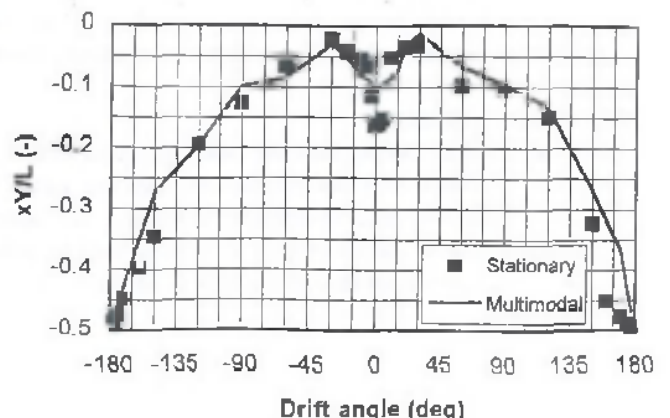


Figure 3: Comparison between the coefficient  $C(\beta)$  resulting from stationary and multimodal tests (GE).





### 3.4. Comparison between test results

A comparison between these two different test techniques for  $Y'(\beta, 0)$ ,  $N'(\beta, 0)$ ,  $C(\beta)$  and  $x_y/L$  is made in figures 1-4 (test condition GE).

No substantial differences between the function elements in expressions (4) and (5) can be observed. Nevertheless, minor differences occur: multimodal tests result into a larger maximum yawing moment compared to stationary tests for pure drift, which implies that the application point of the force  $Y'(\beta, 0)$  moves to the leading edge of the ship model. In general, it can be concluded that non-stationary effects due to the harmonic time history of the applied propeller rate can be neglected.

### 3.5. Limitations

Instabilities were observed in case of backward sailing ( $150 \text{ deg} < |\beta| < 180 \text{ deg}$ ), combined with a positive propeller rate ( $n > 0$ ). This case is comparable with a combination of forward speed and reversed propeller rate ( $u > 0$ ,  $n < 0$ ), which causes an asymmetric flow pattern in the vicinity of the ship's stern, resulting into a lateral force acting to port and a positive yawing moment. In (very) shallow water ( $h/T = 1.1 - 1.2$ ), it appears that this effect is accompanied by unsteady hydrodynamic phenomena, as reported in [3]: although the sign of the average values for  $Y$  and  $N$  indeed confirm the behaviour described above, it was observed that large eddies which are shed from the stern of the model result into slowly fluctuating lateral forces and yawing moments. The amplitude of these oscillations may even exceed the steady term, [4]. Similar phenomena were reported by Ch'ng & Renilson [5], who even observed amplitudes of about 10 times the steady value.

It is clear that such phenomena can impossibly be simulated by means of a quasi-stationary mathematical model, and can only be investigated by captive model tests in which the determining parameters take constant values. Multimodal tests with varying negative propeller rate only produce more complicated non-stationary effects, as shown in figure 5.

### 3.6. Conclusion

It is shown that stationary oblique towing tests and multimodal tests at constant drift angle and harmonically varying propeller rate produce comparable results. Exception should be made for a limited range of small drift angles, where reversed propeller rates cause non-stationary effects.

This equivalence implies that only one run per drift angle is required in order to evaluate forces due to drift at any (positive) propeller rate. One stationary oblique towing test, on the other hand, only leads to information about three

discrete propeller loadings. In case a more detailed assessment is desired, the number of tests has to be doubled at least; if, on the other hand, one run is considered to be sufficient, it cannot be denied that a multimodal run will reveal more useful data.

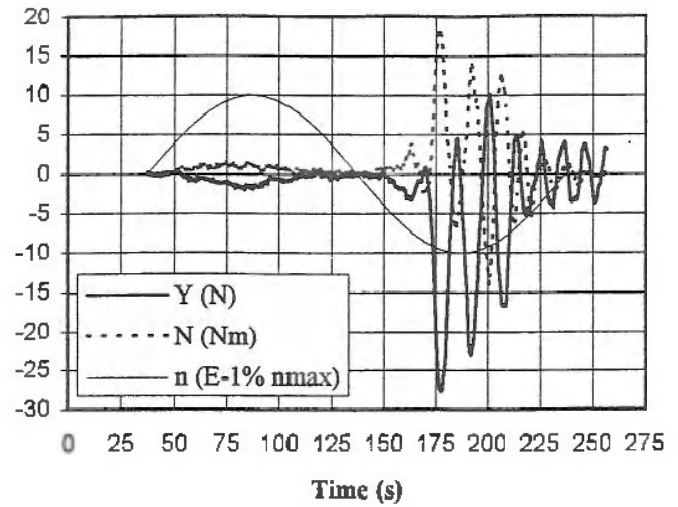


Figure 5: Fluctuating lateral forces and yawing moments observed during a multimodal test with harmonically varying propeller rate (C3).

## 4. VARIABLE DRIFT

### 4.1. Test conditions

An accurate determination of the tabular form for  $Y'(\beta, 0)$  and  $N'(\beta, 0)$  requires at least a series of thirty test runs since each value in the table is obtained from one (stationary or multimodal) oblique towing test.

This time consuming test program could be reduced by introducing a test during which a constant speed of the towing carriage is combined with a yawing motion at constant rate of turn (see figure 6). Actually, such a test can be considered as a multimodal test characterized by:

- a constant yaw velocity  $r$ ;
- harmonically oscillating longitudinal and lateral velocity components  $u(t)$  and  $v(t)$ :

$$\begin{aligned} u(t) &= u_m + u_A \sin(\omega_u t + \phi_u) \\ v(t) &= v_m + v_A \sin(\omega_v t + \phi_v) \end{aligned} \quad (7)$$

with following test parameters:  $\omega_u = \omega_v$ ,  $u_A = v_A$ ,  $|\phi_u - \phi_v| = 90^\circ$  deg, which leads to a constant value for the magnitude of the speed vector  $V$ .

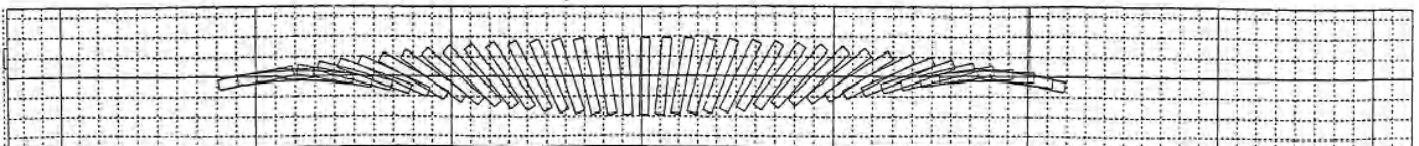


Figure 6: Run I of a multimodal test during which a constant speed of the towing carriage  $V$  is combined with a yawing motion at constant rate of turn  $r$ .

At model scale, the rate of turn is typically 0.5 or 1.0 deg/s, while a very low carriage speed (0.1 - 0.15 m/s) has to be applied if the drift angle has to be varied over four quadrants.

It is clear that test results will differ substantially from those obtained from stationary oblique towing tests, due to several reasons.

- Forces and moments will be affected by yawing, and by interaction between yawing and swaying.
- The acceleration components  $\ddot{u}(t)$  and  $\ddot{v}(t)$  are small but non-zero, so that inertia terms can also influence measured forces and moments.
- Harmonic variation of forward and lateral velocity components may induce non-stationary effects.

For given values of  $V$  and  $r$ , a series composed of four runs is carried out, characterized by different ranges for the drift angle  $\beta$  and the hydrodynamic inflow angle  $\gamma$  (Table 2, figure 7), and yielding two curves for  $Y'$  and  $N'$  as a function of  $\beta$ . The effect of (a) and (b) can be eliminated by considering the average of both curves; comparison with the results of stationary tests allows evaluation of the effect of non-stationary phenomena, (c).

Table 2. Ranges for angles  $\beta$  and  $\gamma$

		$\beta$ (deg)	$\gamma$ (deg)
Run I	$r > 0$	$0 \rightarrow 180$	$0 \rightarrow 180$
Run II	$r > 0$	$-180 \rightarrow 0$	$180 \rightarrow 0$
Run III	$r < 0$	$180 \rightarrow 0$	$-180 \rightarrow 0$
Run IV	$r < 0$	$0 \rightarrow -180$	$0 \rightarrow -180$

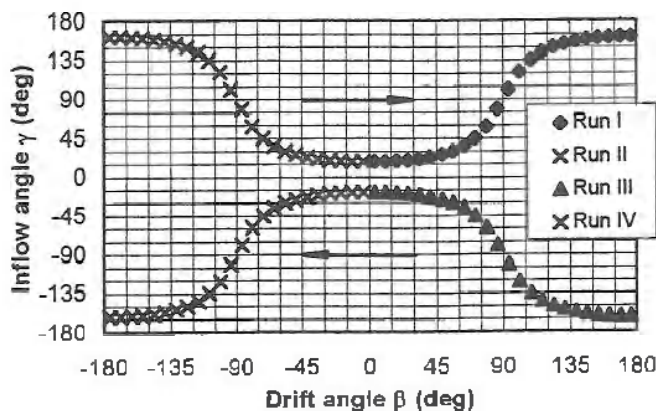


Figure 7: Relationship between hydrodynamic angles  $\beta$  and  $\gamma$  during each test run.

#### 4.2. Test results

Figures 8 and 9 show the measured non-dimensional lateral force and yawing moment as functions of the drift angle  $\beta$  for each run (I to IV), together with the results of stationary oblique towing tests.

In figures 10 and 11, the averages of lateral force and yawing moment measured during port and starboard turns for parametrically comparable runs (runs I-III; runs II-IV) are displayed and compared with results of oblique towing tests.

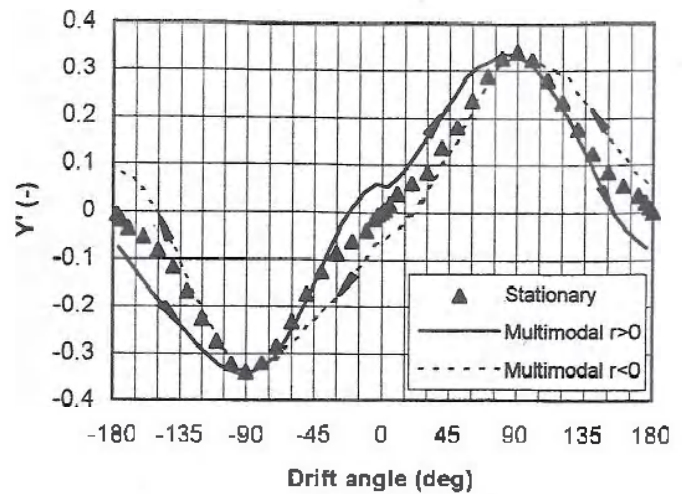


Figure 8: Non-dimensional lateral force  $Y'$  measured during stationary oblique towing tests and non-stationary multimodal tests (C2,  $|r| = 1$  deg/s).

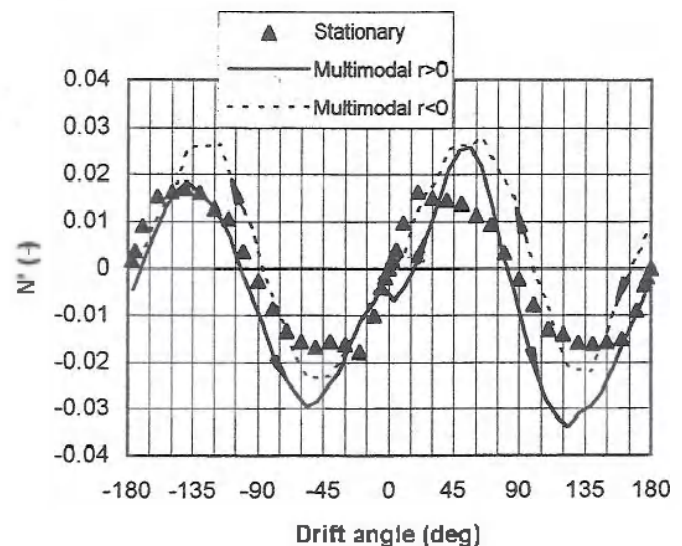


Figure 9: Non-dimensional yawing moment  $N'$  measured during stationary oblique towing tests and non-stationary multimodal tests (C2,  $|r| = 1$  deg/s).

Obviously, results of steady tests do not coincide with the average curve obtained from non-stationary tests. Following differences are observed:

- non-stationary effects are more important at larger drift angles;
- the yawing moment is clearly more affected than the lateral force;
- at rather limited drift angles ( $|\beta| < 20$  deg), forces and moments are slightly larger when measured during oblique towing tests;
- at larger drift angles, non-stationary effects induce a minor increase of lateral force, and a substantial increase of the yawing moment;
- non-stationary effects clearly increase with increasing rate of turn.

Figures 8 to 11 concern one particular test series (C2) with a panamax bulk carrier at 10% under keel clearance, but similar results were obtained with other - both slender (FA) and full (GA) - ship models.



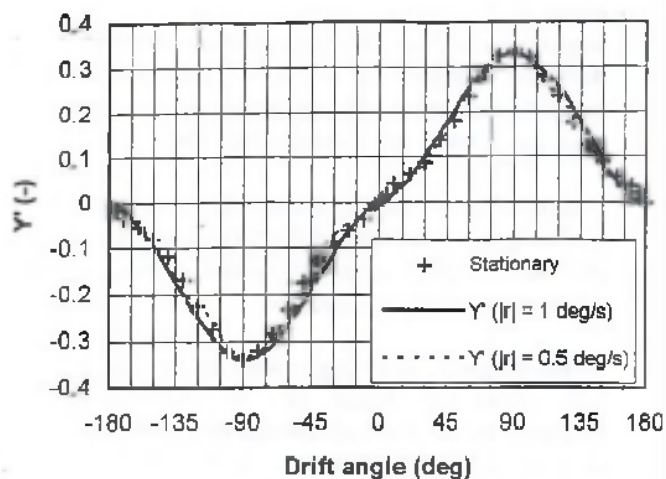


Figure 10: Comparison between the lateral force  $Y'$  measured during stationary oblique towing tests and the mean values for  $Y'$  according to multimodal tests (C2).

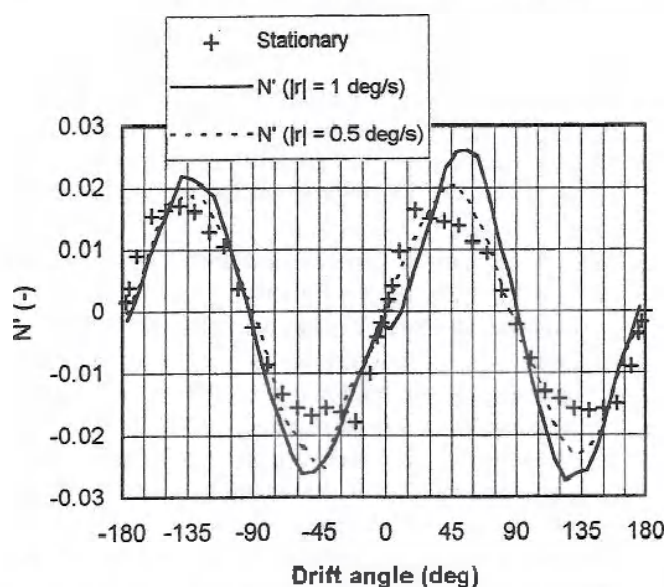


Figure 11: Comparison between the yawing moment  $N'$  measured during stationary oblique towing tests and the mean values for  $N'$  according to multimodal tests (C2).

#### 4.3. Discussion

The phenomena described in 4.2 could be explained as follows.

At lower drift angle, the flow pattern is not fully developed during non-stationary tests, yielding somewhat smaller forces and moments. Comparable conclusions can be formulated if the results of oblique towing tests are compared with the speed-dependent terms of harmonic (PMM) sway tests, [2].

At larger drift angles, however, non-stationary effects apparently induce a stabilizing influence on the flow pattern. Indeed, the maximum yawing moment is obtained at a larger drift angle (20 deg vs. 45-55 deg), while this maximum value is about 50% larger. Apparently, the supplementary yawing motion prevents stall at low drift angle.

#### 4.4. Conclusion

It is clear that the discussed type of non-stationary test cannot reproduce oblique towing test results, as the yawing motion

appears to influence the flow around the ship model substantially.

On the other hand, there is no reason why the results of non-stationary tests would be inferior to those of oblique towing tests. As a matter of fact, in both cases the values for the velocity components imposed to the ship model can be considered to be realistic for tug-assisted ships during harbour manoeuvres. Therefore, the question arises whether it is justified to neglect non-stationary effects by making use of quasi-stationary mathematical models for simulation of certain manoeuvres.

### 5. RUDDER INDUCED FORCES AND MOMENTS

#### 5.1. Stationary rudder angle tests

Lateral force and yawing moment measured during stationary rudder angle tests at maximum rpm are presented in figure 12 and 13 (model C3).

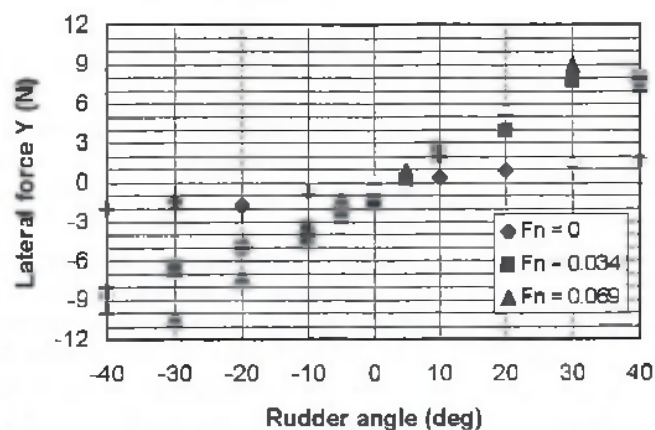


Figure 12: Influence of forward speed  $u$  on lateral force  $Y$  during stationary rudder angle tests at maximum rpm (C3).

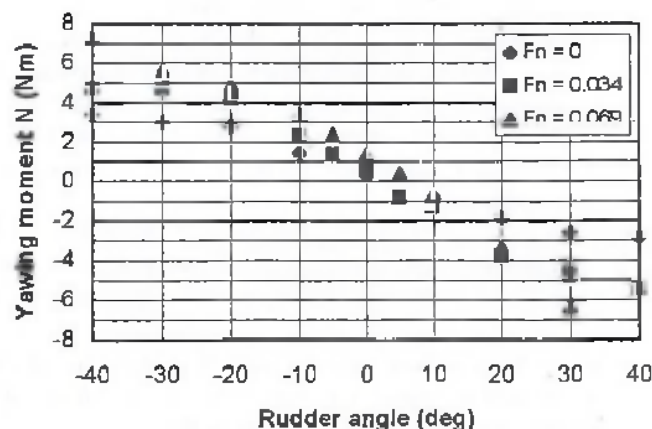


Figure 13: Influence of forward speed  $u$  on yawing moment  $N$  during stationary rudder angle tests at maximum rpm (C3).

The influence of the forward speed  $u$  on  $Y$  and  $N$  can be explained as follows [4],[6]: at bollard pull, forces due to rudder action are concentrated on the rudder, which is situated in the propeller slipstream. At non-zero forward speed, the flow around the hull is influenced by the asymmetry due to the rudder deflection, so that an additional lateral force applies on the hull. The rudder module proposed by Group-MMG is based on this analysis, [7]:

$$Y = (1 + a_H) Y_R \quad (8)$$

$$N = Y_R x_R + a_H Y_R x_H$$

$Y_R$  being the force acting on the rudder,  $a_H$  the ratio between lateral forces on rudder and hull,  $x_H$  and  $x_R$  the longitudinal position of the application point of the force acting on the hull and the rudder, respectively.

At zero rudder angle, a negative force  $Y$  and positive moment  $N$  occur due to the asymmetrical flow pattern caused by a propeller turning to the right.

### 5.2. Multimodal rudder angle tests

The interaction between hull, propeller and rudder can principally be assessed by means of several types of multimodal tests, subdivided according to the number and type of oscillating test parameters, see Table 3.

Table 3. Multimodal rudder angle tests.

Type	forward velocity $u$	propeller rate $n$	rudder angle $\delta$
I	constant	constant	harmonic
II	constant	harmonic	harmonic
III	harmonic	constant	harmonic

Before comparing results of multimodal and stationary rudder angle tests, some indication about the non-stationary character of measurements of multimodal test results will be provided. Figures 14 and 15 display the time history of the total lateral force  $Y$  and lateral rudder force  $Y_R$  measured during type I tests, carried out at zero and non-zero forward speed, respectively. Following conclusions can be formulated.

- At both speeds, a periodical time history is obtained for the force acting on the rudder, so that the latter does not appear to suffer from memory effects.
- In bollard pull conditions, the lateral force acting on the hull is affected substantially by non-stationary effects induced by the permanent action of the propeller. A lateral force acting to port is developed during the test, which dominates the rudder induced force after about three oscillations.
- At non-zero forward speed, the total lateral force is hardly affected by memory effects: the measured force does not change significantly during subsequent oscillation cycles.

It can be concluded that an increasing model speed leads to an important stabilizing effect on the asymmetrical flow pattern generated around the ship model.

In order to exclude the influence of memory effects as much as possible, the evaluation of the similarity between the results of stationary and multimodal tests will be based on forces and moments measured during the first oscillation cycle, unless a clear periodicity is observed.

### 5.3. Comparison between stationary and multimodal tests

*Test type I - Zero speed.* Figures 16-17 display results for model test series DB, measured in bollard pull conditions with propeller full ahead. The results for the lateral force  $Y_R$  on the rudder are practically identical, but multimodal tests

appear to overestimate the lateral force  $Y$  for negative rudder angles (figure 16). This implies that, for rudder actions to starboard, a larger value for the hull force ratio  $a_H$  is obtained by means of multimodal test results; stationary tests, on the other hand, result into a value for  $a_H$  which is about zero.

Compared to the results of stationary tests, multimodal tests lead to an overestimation of the yawing moment  $N$  (figure 17) for the complete range of rudder angles, although the difference is larger at negative  $\delta$ .

As the negative rudder angles were applied during the second half period (see figure 14), the discrepancies may be explained by the effect of non-stationary phenomena induced by the continuous propeller action. As a reference, a stationary test typically takes 40 s.

*Test type I - Non-zero speed.* An increasing forward velocity leads to a better agreement between results of stationary and multimodal tests, although the possible influence of non-stationary phenomena must constantly be born in mind.

*Test type II - Non-zero speed.* Model C3 was subjected to stationary rudder angle tests and a multimodal test with variable rudder angle and propeller rate at a constant model speed ( $F_n=0.052$ ). The multimodal test was executed with test periods  $T_\delta$  and  $T_n$ , respectively 1/2 and 1/5 of the total test time. A comparison between measured forces and moments leads to the following observations:

- lateral rudder force  $Y_R$  does not differ substantially;
- lateral force  $Y$  and yawing moment  $N$  are affected in an opposite way, so that force  $Y$  is underestimated for almost all combinations ( $\delta, n$ ) resulting into a minor fraction  $a_H$ , and moment  $N$  is mainly overestimated which implies that the coordinate  $x_H$  of the additional lateral force moves towards the stern compared to stationary tests.

This phenomenon can possibly be ascribed to the fact that during non-stationary tests the flow pattern around the hull is not fully developed.

*Test type III - Harmonically varying speed.* A multimodal test with harmonically varying speed and rudder angle and a constant propeller rate generates dynamic effects which influence forces and moments in a same way as non-stationary tests of type II do. Figure 18 (condition C3) illustrates the reduced ratio  $a_H$  measured for rudder deflections within the range [30 deg ; 40 deg]. The lines representing the results from stationary tests are based on following equation, [6]:

$$a_H = \frac{\lambda(\delta) \left( \frac{u}{nD} \right)}{\left( \frac{u}{nD} \right)^3 + \theta(\delta)} \quad (9)$$

Near bollard pull condition, ratio  $a_H$  takes non-zero values. This effect was also observed during multimodal test of type I at zero speed. The scatter on the test results increases with decreasing propeller loading due to a reduced rudder action. The expected maximum value is about 70 to 80% of the fraction  $a_H$  resulting from stationary rudder angle tests.



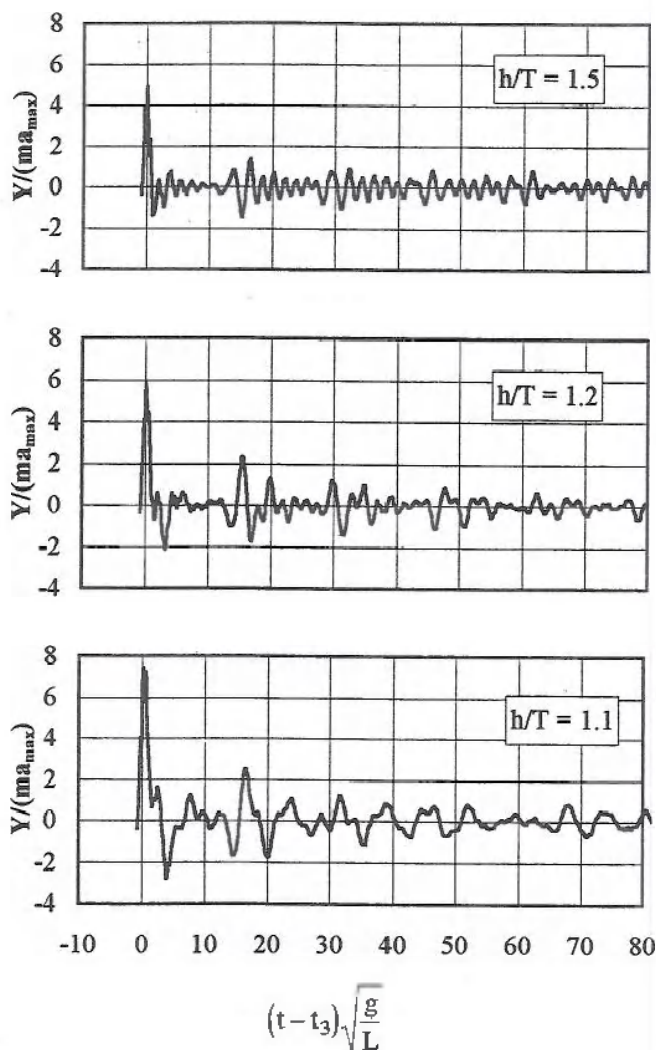


Figure 3. Captive quay wall approach tests with panamax bulk carrier model ( $q_M/B = 0.1$ ,  $u = 0$ ,  $n = 0$ ): lateral force during and after deceleration test. Influence of water depth.

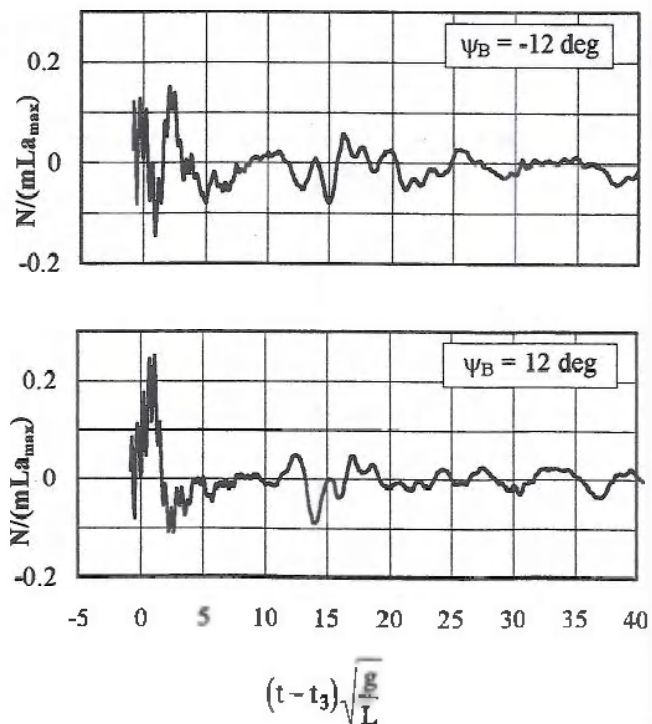


Figure 5. Captive quay wall approach tests with panamax bulk carrier model ( $q_M/B = 1.0$ ,  $h/T = 1.2$ ,  $u = 0$ ,  $n = 0$ ): yawing moment during and after deceleration test. Influence of orientation with respect to quay wall.

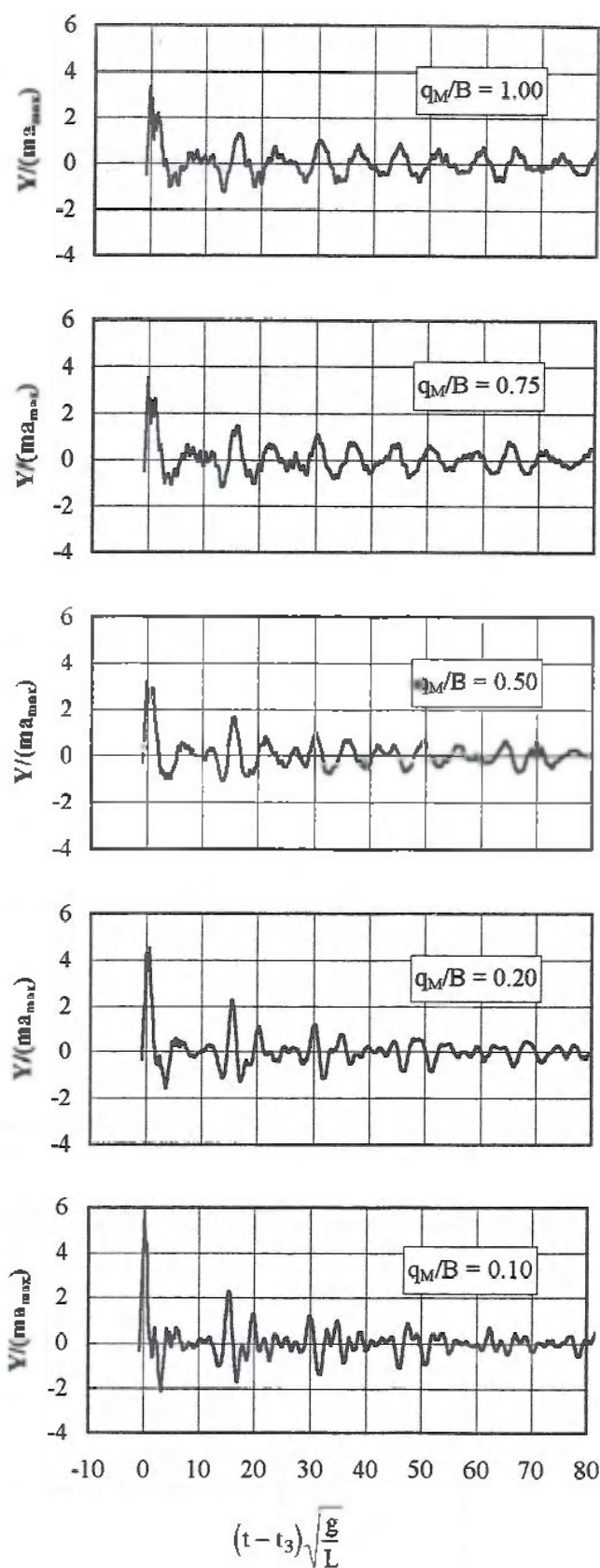
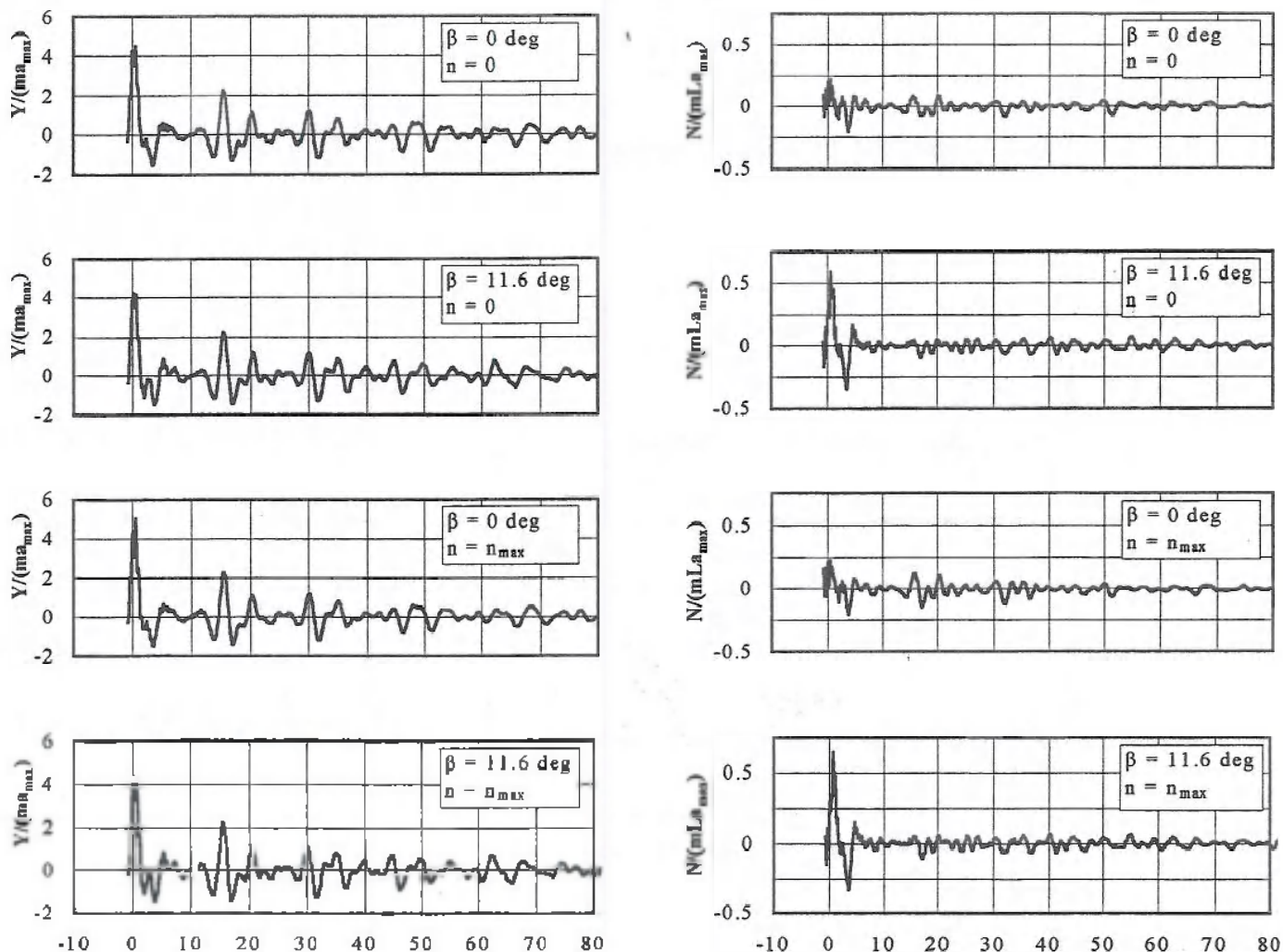


Figure 4. Captive quay wall approach tests with panamax bulk carrier model ( $h/T = 1.2$ ,  $u = 0$ ,  $n = 0$ ): lateral force during and after deceleration test. Influence of quay clearance.

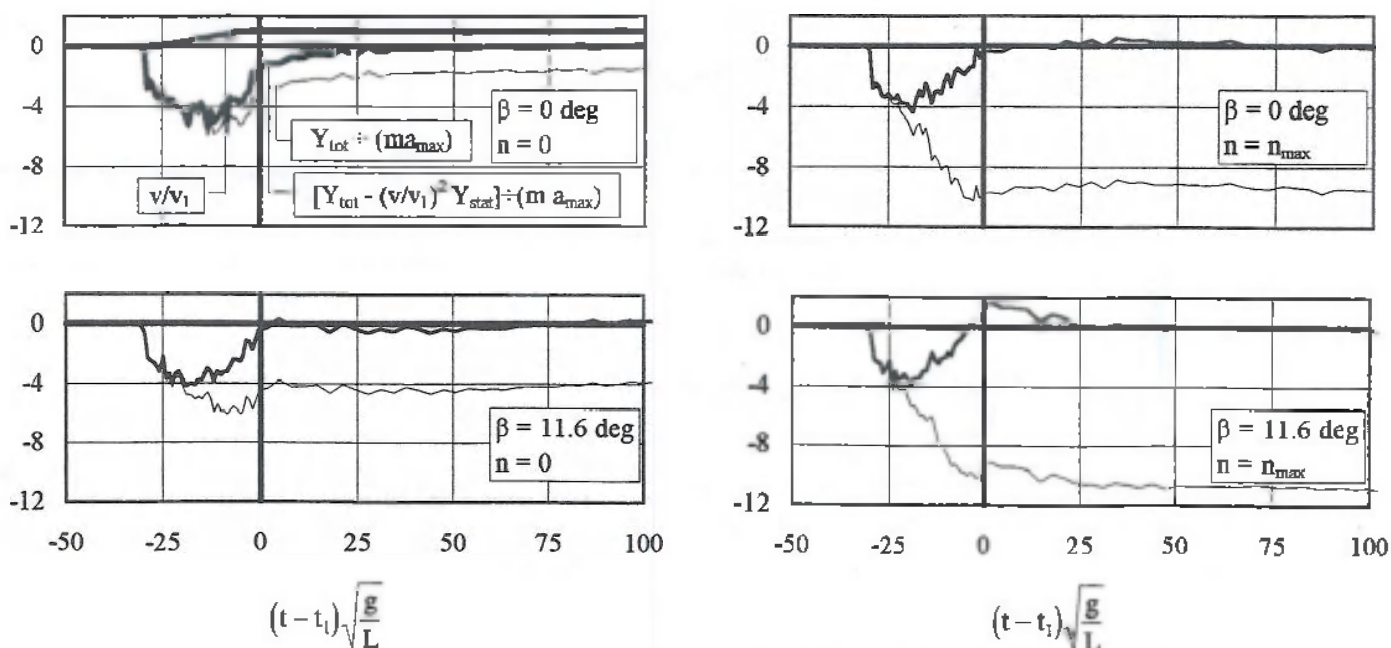




$$(t - t_3) \sqrt{\frac{g}{L}}$$

$$(t - t_3) \sqrt{\frac{g}{L}}$$

Figure 6. Captive quay wall approach tests with panamax bulk carrier model ( $q_M/B = 0.2$ ,  $h/T = 1.2$ ,  $\psi_B = 0$  deg): lateral force and yawing moment during and after deceleration phase. Influence of forward speed and propeller rate during steady phase.



$$(t - t_1) \sqrt{\frac{g}{L}}$$

$$(t - t_1) \sqrt{\frac{g}{L}}$$

Figure 7. Captive quay wall approach tests with panamax bulk carrier model ( $h/T = 1.2$ ): lateral force during and after acceleration phase. Influence of forward speed and propeller rate during steady phase.

$$\begin{aligned}
K^{(j)}(t) &= \xi^{(j)} B_1^{(j)} e^{-\alpha^{(j)} t} \left( \cos \omega_0^{(j)} t - \frac{\alpha^{(j)}}{\omega_0^{(j)}} \sin \omega_0^{(j)} t \right) \text{ if } A_0^{(j)} - \alpha^{(j)^2} > 0 \\
&= \xi^{(j)} B_1^{(j)} e^{-\alpha^{(j)} t} (1 - \alpha^{(j)} t) \text{ if } A_0^{(j)} - \alpha^{(j)^2} = 0 \\
&= \xi^{(j)} B_1^{(j)} e^{-\alpha^{(j)} t} \left( \cosh \omega_0^{(j)} t - \frac{\alpha^{(j)}}{\omega_0^{(j)}} \sinh \omega_0^{(j)} t \right) \text{ if } A_0^{(j)} - \alpha^{(j)^2} < 0
\end{aligned} \quad (8)$$

where

$$\alpha^{(j)} = \frac{1}{2} A_1^{(j)} \quad (9)$$

$$\omega_0^{(j)^2} = \left| A_0^{(j)} - \alpha^{(j)^2} \right| \quad (10)$$

The transfer function parameters  $\xi^{(j)}$ ,  $A_0^{(j)}$ ,  $A_1^{(j)}$ ,  $B_1^{(j)}$  ( $j=1,2$ ) depend on the position of the ship referred to the quay wall, i.e. on distance and orientation. An algorithm has been developed for an optimal determination of these parameters if the added mass and hydrodynamic damping coefficients are known functions of frequency.

### 3.2. Experimental observations

**General considerations.** Analysis of the results of the captive model tests described in paragraph 2.1 leads to a better qualitative understanding of the significance of the parameters determining non-stationary forces and moments acting on a ship model in a non-steady motion. Following parameters will be considered: water depth ( $h/T$ ), average quay clearance ( $q_M/B$ ), orientation with respect to the bank, drift angle ( $\beta$ ), propeller action. Both the acceleration and deceleration phases will be discussed, although non-steady phenomena can be observed more clearly during the latter, due to the larger acceleration magnitudes experienced by the ship model. Moreover, the quay clearance parameter was only varied systematically during the deceleration phase.

**Water depth.** Figure 3 shows the influence of  $h/T$  on the time record of the lateral force acting on the decelerating ship model. It is clear that the under keel clearance significantly affects the magnitude of the extrema, as well as their time of occurrence. Dominating frequencies appear to decrease with decreasing water depth.

**Average quay clearance.** As expected, the distance from the ship's side to the quay wall is a significant parameter. Figure 4 shows that dominating frequencies increase with decreasing quay clearance, while the magnitude of the extrema increases. This effect becomes significant for quay clearance values smaller than half the ship's beam.

**Orientation with respect to the bank.** The angle between the quay wall and the ship's longitudinal axis of symmetry does not appear to have significant influence on the lateral force. The effect on the yawing moment, on the other hand, can be observed very clearly (figure 5): nonzero values for  $\psi_B$  result into additional damped oscillating time functions.

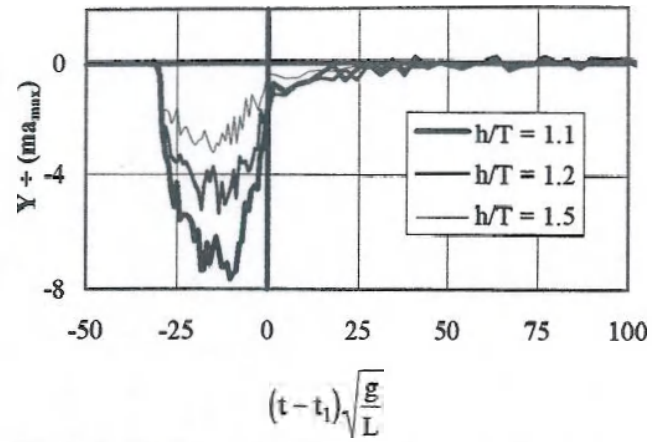


Figure 8. Captive quay wall approach tests with panamax bulk carrier model ( $\beta = 0$ ,  $n = 0$ ): lateral force ( $Y / ma_{max}$ ) during and after acceleration phase. Influence of water depth.

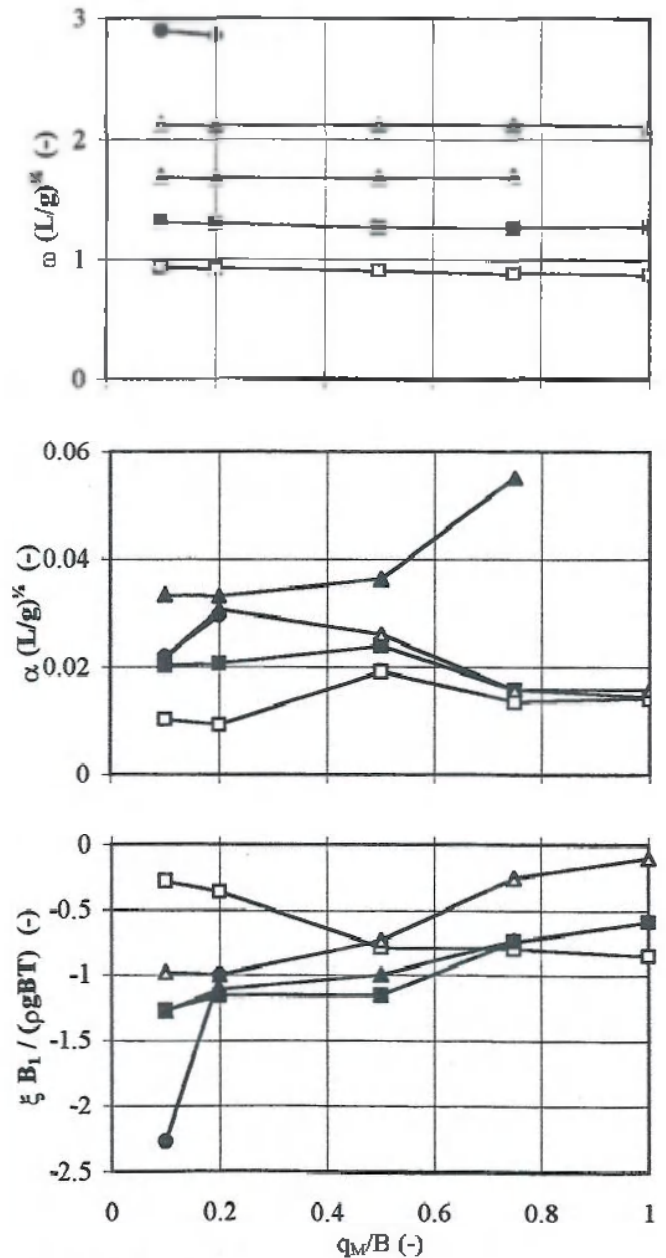


Figure 10. Captive quay wall approach tests with panamax bulk carrier model ( $u=0$ ,  $n=0$ ,  $h/T = 1.2$ ). Lateral force due to lateral motion: influence of quay clearance on transfer function parameters.